Progress In Electromagnetics Research, Vol. 117, 1–18, 2011

A LATE-TIME ANALYSIS PROCEDURE FOR EXTRACTING WEAK RESONANCES. APPLICATION TO THE SCHUMANN RESONANCES OBTAINED WITH THE TLM METHOD

J. A. Morente

Department of Applied Physics
University of Granada, Granada E-18071, Spain

E. A. Navarro

Department of Applied Physics
University of Valencia, Burjassot, Valencia E-46100, Spain

J. A. Portí

Department of Applied Physics
University of Granada, Granada E-18071, Spain

A. Salinas

Department of Electromagnetism and Material Physics
University of Granada, Granada E-18071, Spain

J. A. Morente-Molinera

Higher Technical School of Information Technology and Telecommunications Engineering
University of Granada, Granada E-18071, Spain

S. Toledo-Redondo

Department of Electromagnetism and Material Physics
University of Granada, Granada E-18071, Spain

W. J. O'Connor

School of Electrical, Electronic and Mechanical Engineering
University College Dublin, Belfield, Dublin 4, Ireland

Received 4 April 2011, Accepted 9 May 2011, Scheduled 25 May 2011
Corresponding author: Juan Antonio Morente (jmorente@ugr.es).

B. P. Besser and H. I. M. Lichtenegger

Space Research Institute
Austrian Academy of Sciences
Schmiedlstrasse 6, Graz A-8042, Austria

J. Fornieles and A. Méndez

Department of Electromagnetism and Material Physics
University of Granada, Granada E-18071, Spain

Abstract—The sequence of Schumann resonances is unique for each celestial body with an ionosphere, since these resonances are determined by the dimensions of the planet/satellite and the corresponding atmospheric conductivity profile. Detecting these frequencies in an atmosphere is a clear proof of electrical activity, since it implies the existence of an electromagnetic energy source, which is essential for their creation and maintenance. In this paper, an analysis procedure for extracting weak resonances from the responses of electromagnetic systems excited by electric discharges is shown. The procedure, based on analysis of the late-time system response, is first checked using an analytical function and later applied to the vertical electric field generated by the computational simulation of Earth's atmosphere using the TLM (Transmission Line Matrix) method in order to extract the weak Schumann resonances contained in this electric field component.

1. INTRODUCTION

Solar photons and galactic cosmic rays penetrating the upper layers of Earth's atmosphere, aerosol populations and radon emanating from the land surface increase the ionization and contribute to forming an electrical conductivity profile [1, 2] that, starting from low values near the surface, rises with altitude and generates an electromagnetic cavity for waves propagating in the ELF-VLF range [3, 4]. This natural cavity is excited, basically, by the 2,000 permanently active thunderstorm cells worldwide which produce approximately 50 lightning events every second [5], although volcanic eruptions, dust storms and tornadoes can also be seeds of electromagnetic signals [6]. Most of the electromagnetic energy produced by these natural events is radiated around 3 kHz in the VLF band, although they are transient signals with a broadband spectrum. During their propagation, the radio waves trapped in the cavity must adapt to its geometrical form, which is strongly dispersive

and greatly distorts the waveform of the excitation signal, allowing effective propagation of only those frequencies around the resonance frequencies of the different modes at which the cavity resonates. Any electromagnetic perturbation in the spherical shell cavity formed by the ground, the conducting ionosphere and the atmosphere between them can be described as a superposition of TE^r modes (electric field transverse to the radial direction r) with non-zero field components H_r, H_ϑ, and E_φ, and TM^r modes (transverse magnetic with respect to r) with E_r, E_ϑ, and H_φ components. The TEM modes are excluded because they represent the static solution, taking the form of a plane wave without cutoff or resonance frequencies. Following the notation given in [7], with the script n and m as indices for the associated Legendre functions or spherical harmonics and with the script p indicating the successive zeroes of the spherical Bessel function of order n in the TE^r modes, or its derivative for TM^r modes, all the TE^r_{mnp} modes and the TM^r_{mnp} with $p \neq 1$ are called transverse resonances [8–10]; they fall almost entirely within the VLF band, with half-wavelengths proportional to the distance between the ground and the ionosphere, and are local phenomena because their energy remains concentrated around the excitation source [11, 12]. However, the TM^r_{mn1} modes, known as Schumann resonances [13, 14], are modes globally coupled with the Earth-ionosphere cavity that should be detected anywhere on Earth and their resonant frequencies are in the ELF band. The propagation of ELF-VLF radio waves in the terrestrial atmosphere has been widely studied, due to its importance in communication and navigation systems. Here, we would like to highlight the books of Wait [15], Budden [16], and Nickolaenko and Hayakawa [17].

The idea that the Earth-ionosphere cavity would support electromagnetic standing waves was predicted by Schumann in 1952 [13] and detected experimentally in 1960 by Balser and Wagner [18], who identified the first five Schumann resonant frequencies. Nowadays, there is a renewed interest in the Schumann resonance signals since Williams [19] observed, for a period of six years, a correlation between variations in the tropical temperature and variations in the lowest Schumann-resonance-mode intensity. This correlation led him to suggest that these resonances could be used as a global thermometer for the tropics of the Earth, since the worldwide lightning-flash rate, source of the Schumann resonances, is dependent on the average global temperature. The Schumann resonances, contained in the TM^r_{mn1} modes, are practically quasi-TEM modes because the electric tangential component is much lower than the radial electric field in the cavity [20] and, moreover, its

amplitude must be close to zero near the two spherical external surfaces because the boundary conditions impose a vanishing tangential electric field on the conducting surfaces. Regarding their frequency and field amplitude, the first six experimental Schumann resonances are observed at nominal frequencies of 7.8, 14, 20, 26, 33, and 39 Hz, with a variation in these values of ± 0.5 Hz, and their amplitudes are in the picotesla range for the magnetic field and around tenths of a millivolt for the electric field [3]. So, the Schumann resonances are extremely weak compared with the ambient geomagnetic field and with the static electric field generated by thunderstorms which maintain a potential difference between the ionosphere and the ground of approximately 300 kV with a 120 V/m electric field at ground level [21]. In this paper, a computational simulation of Earth's ionosphere using the TLM method is carried out in order to obtain the Schumann resonance spectra. By including in the numerical algorithm a model for the conductivity profile in the Earth's atmosphere, a resonant spectrum is obtained for the tangential magnetic field with peak values close to the experimental ones. However, the capacitive effect of the two conducting surfaces, which define the electromagnetic cavity, and the assumption of a vertical electric dipole as excitation source, determine a radial electric field with a high DC component that hides the Schumann resonances in the electric field spectrum, thus a post-processing analysis of these data being required to recover these resonances. To deal with this situation, thus a procedure is developed for extracting weak resonances from the responses of electromagnetic systems excited by electric discharges. The procedure, based on analysis of the late-time system response, is first checked using an analytical function and later applied to the data of the vertical electric field generated by the computational simulation of Earth's atmosphere using the TLM method.

The TLM method provides a different approach from that supplied by the more popular FDTD (finite differences in the time domain) method for a numerical analysis of the Earth-ionosphere cavity [22–24] or other electromagnetic systems [25, 26]. Although both are low-frequency methods and need spatial and temporal discretization, they are conceptually different. For example, TLM has been used to model challenging situations such as radiation by thin conducting wires with a radius much smaller than the mesh size by simply including a transmission line circuit describing the inductance and capacitance introduced by the wire to the medium in which it is placed [27]. Another advantage of TLM over FDTD is that TLM defines all the field quantities at the same point, the center of the node, as well as all the perpendicular field quantities at the interface between nodes,

which simplifies the imposition of boundary conditions. In contrast, although FDTD is computationally more economical, it defines each component of the electromagnetic field at a different point and even at a different time, which complicates the task of accurately defining the transition between different media.

2. EARTH'S RESONANT CAVITY FOR ELF ELECTROMAGNETIC WAVES

The electromagnetic wave propagation of atmospheric signals in the ELF range associated with the Schumann resonances can be modeled by considering the system as an inhomogeneous lossy cavity formed by two conducting spherical surfaces. This is justified by the relatively high conductivity values on the ground's surface, around 4 S/m for seawater and from 10^{-3} to 10^{-5} S/m for the solid surface, and on the strong increase in atmospheric conductivity, which changes from 10^{-14} S/m near ground level to 10^{-3} S/m at a height just below 100 km, with an appreciable increment in the slope at an altitude of around 60 km [28], as is shown in Figure 1. With these values, at 25 Hz, a frequency in the middle of the range of interest, the ratio between the displacement and conductivity current, $\omega\varepsilon_0/\sigma$, is 1.4×10^5 at ground level and 1.4×10^{-6} at a height of 100 km; consequently, the atmosphere behaves like a dielectric with low losses at ground level to become a good conductor for higher regions.

As an alternative, the reflection coefficient Γ can give a clear graphic vision of the Earth's cavity, besides being useful in the later implementation of the TLM numerical algorithm. Let us consider the

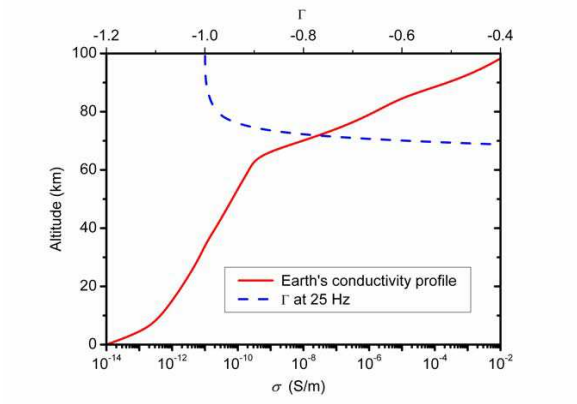

Figure 1. Conductivity and real part of the reflection coefficient profiles in the Earth's lower atmosphere.

normal reflection of a plane wave at a metallic boundary. The wave is usually reflected almost completely, and for a perfect conductor with infinite conductivity, the transmission is zero since there can be no electromagnetic field inside a perfect conductor. However, for a metal of finite conductivity σ, its impedance is given by $Z_c = Z_0\sqrt{j\omega\varepsilon_0/\sigma}$, where Z_0 is the characteristic impedance for the free space, and Γ can be expressed as [29]

$$\Gamma = \frac{Z_c - Z_0}{Z_c + Z_0} = \frac{\sqrt{j\omega\varepsilon_o/\sigma} - 1}{\sqrt{j\omega\varepsilon_0/\sigma} + 1} \simeq -1 + \sqrt{\frac{\omega\varepsilon_0}{2\sigma}}. \tag{1}$$

In the above equation, for the latter approach, the imaginary part of Γ is negligible and Γ becomes a real value. For the interface atmosphere-seawater, $\Gamma = -0.999987$ at 25 Hz, and for solid ground with $\sigma = 10^{-3}$ S/m, $\Gamma = -0.9992$. Figure 1 also shows this reflection coefficient for a 25 Hz electromagnetic wave incident from the free space in a dissipative medium with a conductivity $\sigma(z)$ given by the Earth's profile. In this figure, Γ is very close to -1 at a height of 100 km, this value indicating that such a distance is a good choice for locating the external conducting surface of the Earth-ionosphere cavity.

3. MODELING OF THE EARTH-IONOSPHERE CAVITY FOR SCHUMANN RESONANCES WITH THE TLM METHOD

The Transmission Line Matrix (TLM) numerical method is an approach, devised in the time domain, to the computer simulation of propagation and diffusion processes [27, 30]. For electromagnetic waves, the TLM method sets up an iterative process which allows the temporal evolution of the six electromagnetic field components to be obtained. It is based on the construction of a three-dimensional transmission line mesh formed by interconnecting unitary circuits termed nodes or cells. Each node in the mesh has associated with it a matrix S built with Maxwell's equations so that voltages and currents in this mesh behave similarly to the electromagnetic field in the original system. To be specific, in this paper, the three-dimensional condensed node with spherical geometry is used [31]; however, independently of the specific node used, the basis of the TLM algorithm is quite simple. Along with the spatial discretization associated with the TLM node mesh, a temporal discretization coordinated with the spatial one is necessary. At time step n, $t = n\Delta t$, a set of voltage pulses represented by a column matrix V_n^i are incident at each node in the TLM mesh, which after scattering at each node center, produce a set of reflected pulses represented by a column matrix V_n^r. The two pulse sets are

related by the scattering matrix of the node S by equation $V_n^r = SV_n^i$. Reflected pulses propagate through all the lines in the nodes and become incident pulses at neighbor nodes for the next time step. For lossy systems, S is a 21×21 square matrix whose elements are related to the dimensions of the elementary volume modeled by the node and to the electric permittivity, magnetic permeability and conductivity of the medium to be simulated [32].

In order to make an efficient TLM mesh to study the Schumann resonances in Earth's ionosphere, several considerations should be kept in mind, such as the size of the mesh, the excitation and the external boundary. The electromagnetic cavity of our planet has a behavior similar to a microwave cavity except that because of its dimensions; thus, Schumann resonant frequencies are located in the ELF band instead of the microwave zone. Regarding the mesh size or longest dimension of a TLM node, as is well-known in low-frequency numerical methods, a wavelength must be sampled at least eight or ten times. When in the absence of a source term, the cavity resonances are estimated solving the homogeneous wave equation, due to the spherical symmetry of the Earth-ionosphere cavity, the resonances obtained are only functions of the Earth's radius, r_0, and the height of the ionosphere above the ground, h, and do not depend on the zenithal and azimuthal coordinates, θ and ϕ, respectively. The inclusion of the excitation signal in the physical system can break this symmetry; however, if the electromagnetic field source is an electric discharge at the angular coordinates θ and ϕ, it is always possible to choose another system of spherical coordinates with the excitation located in the origin of the θ coordinate (Figure 2). In this specific coordinate system, the resonant cavity plus the electric discharge source form a physical system which is not dependent on the azimuthal coordinate ϕ,

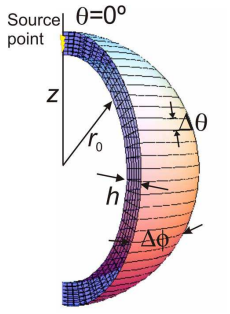

Figure 2. Geometry and coordinates in the TLM mesh to model the Earth-ionosphere electromagnetic cavity.

becoming therefore a two-dimensional system, which can be described by using the coordinates r and θ only. This kind of situation is frequently invoked because a common excitation source in the Earth-ionosphere cavity is cloud-to-ground lightning, which can be described by a radial current and which is a much more efficient excitation of the cavity than horizontal lightning [11]. In our case, the TLM mesh used is 10×36 nodes wide in the r and θ directions. This mesh models an atmosphere with $h = 100\,\mathrm{km}$, which means that $\Delta r = 10\,\mathrm{km}$ and $\Delta\theta = 5^\circ$, and optimum time steps of $\Delta t = 3.48 \times 10^{-6}\,\mathrm{s}$ and $\Delta\phi = 24^\circ$ are chosen to minimize dispersion errors [32].

Regarding the excitation, the lightning discharge process is very complex; however, although earlier processes may radiate some energy, the emission of electromagnetic energy is dominated by the lightning return stroke. In this paper, the exciting electric discharge is assumed to be a broadband signal with a current modeled by a double exponential,

$$i(t) = I_0 \left(e^{-\frac{t}{\tau_1}} - e^{-\frac{t}{\tau_2}} \right) \Theta(t), \tag{2}$$

with $I_0 = 20\,\mathrm{kA}$, $\tau_1 = 10^{-4}\,\mathrm{s}$, $\tau_2 = 5 \times 10^{-6}\,\mathrm{s}$, and where $\Theta(t)$ is the Heaviside unit or step function. This model is usually chosen to represent the current flowing during a return stroke [33, 34]. With the typical parameters used previously, the peak current is 16 kA and the transferred charge $q_0 = I_0(\tau_1 - \tau_2) \approx I_0\tau_1$ is 2 C. Although a vertical cloud-to-ground single-stroke flash and its image, given by a quasi-perfect conducting ground, can exceed a length of 10 km [33, 34], the large dimensions of the system and a current that can be approximated by an instantaneously uniform current from the ground to the return stroke tip [34] allow us to model the excitation discharge as a Hertzian electric dipole. For an arbitrary temporal current shape, the electromagnetic radiation fields of a Hertzian electric dipole, placed along the z-axis, are given by [35]

$$\vec{E}(\vec{r}, t) = \frac{L}{4\pi\varepsilon_0 c^2 r} \frac{d[i]}{dt} \hat{r} \times (\hat{r} \times \hat{z}), \tag{3}$$

$$\vec{H}(\vec{r}, t) = \frac{L}{4\pi c r} \frac{d[i]}{dt} \hat{z} \times \hat{r}, \tag{4}$$

where L is the dipole length and the rectangular brackets denote that the variable contained within them should be evaluated at the retarded time $t' = t - R/c$, with R the distance between field and source point. The instantaneous power $P(t)$ crossing a surface s of any sphere of radius r in the radiation zone, centered on the ground between the lightning channel and its image, is given by integrating the Poynting

vector $\vec{E} \times \vec{H}$ over the surface:

$$P(t) = \int_{\phi=0}^{2\pi} \int_{\theta=0}^{\pi/2} \left(\frac{L \sin\theta}{4\pi c r}\right)^2 Z_0 \left(\frac{d[i]}{dt}\right)^2 r^2 \sin\theta d\theta d\phi$$
$$= \frac{Z_0 L^2}{12\pi^2 c^2} \left(\frac{d[i]}{dt}\right)^2. \quad (5)$$

Hence, the total energy crossing the sphere can be calculated by integrating the instantaneous power over the time. Using the current given in (2), we obtain

$$W = \int_{t=0}^{\infty} P(t)dt = \frac{Z_0 L^2 I_0^2}{24\pi^2 c^2} \frac{(\tau_1 - \tau_2)^2}{\tau_1 \tau_2 (\tau_1 + \tau_2)} \simeq 1.22 \times 10^5 J. \quad (6)$$

The part of this energy that would enter the space simulated by the TLM mesh, that is, $\Delta\phi/2\pi$, is introduced into the mesh through the line 1 of the TLM node (1, 1), placed in the polar position. With regard to how the energy is introduced into the mesh, a broadband signal with a relatively flat spectrum is necessary in order to excite all the resonances equally; however, fulfilling the previous conditions, the mathematical shape is quite irrelevant since any shape would generate similar spectra. In this paper, a voltage pulse with a width Δt and the energy given by (6) is the input signal at $t = 0$. A total of $N = 3 \times 10^6$ time step calculations were carried out, allowing the signal to cover Earth's perimeter more than 70 times, with reflections on the external boundaries controlled by the value of the reflection coefficient at 25 Hz, a frequency in the middle of the interest band. The reflection coefficient Γ defined in (1) is introduced for two reasons: firstly, because this coefficient shows the altitude of the external boundary in a simple graphic form; and secondly, more important in the TLM method, because this coefficient is used in a natural way to implement simple and efficient boundaries in cases where the external surfaces are conducting boundaries but not perfect conductors. Figure 3 shows the spectra of the vertical component of the electric field and the horizontal component of the magnetic field, obtained via a discrete Fourier transform (DFT) of the temporal signals at node (1, 6) of the TLM mesh, i.e., at $\theta = 30°$. With the time step used and the temporal iteration number, the frequency step is $\Delta f = (N\Delta t)^{-1} = 0.096$ Hz. As can be observed in Figure 3, the magnetic field spectrum responds like a damped resonant signal but the continuous level representing the static field and the low-frequency TEM modes mask the resonances of the electric field spectrum. Since each resonant mode in a Schumann power spectrum can be approximated by a Lorentzian function [36, 37], the magnetic resonant spectrum can be expressed approximately as a superposition of Lorentzian functions obtained by least-squares

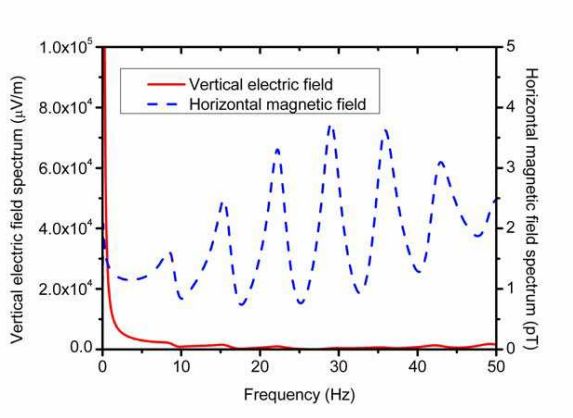

Figure 3. Spectrum of the horizontal magnetic field and vertical electric field in the Schumann resonance band.

Table 1. Experimental and numerical Schumann resonances in the Earth-ionosphere electromagnetic cavity.

n	1	2	3	4	5	6
Experimental Schumann resonances (f, Hz) [3]	7.8	14	20	26	33	39
TLM resonances for horizontal magnetic field (f, Hz)	8.2	15.2	22.0	29.0	35.9	42.9
TLM resonances for vertical electric field (f, Hz)	8.6	16.2	22.3	27.4	35.1	42.4

fitting. The peak frequencies of this fit together with the experimental values [3] are included in Table 1.

4. ANALYSIS PROCEDURE FOR EXTRACTING RESONANCE FREQUENCIES FROM THE LATE-TIME SIGNAL

The late-time unforced transient response of an electromagnetic system excited by an electromagnetic pulse can be written as a series of natural oscillation modes expressed as the product of sine and decreasing exponential functions [38]. Therefore, at the first time as an example,

let us consider the following time-varying function:

$$g(t) = e^{-2\times 10^4 (t-0.2)^2} + 10^{-3}\left[\sin(2\pi \cdot 10 \cdot t) + \sin(2\pi \cdot 30 \cdot t)\right] e^{-2t}, \quad (7)$$

where the amplitude of the sine functions representing the system response is a thousand times lower than the maximum value of the excitation pulse and the decreasing exponential is the term representing the loss in the damped system. Although the exciting pulse and the subsequent response of the system may be repeated periodically, for example, two pulses and system responses are shown in Figure 4(a), the analysis is reduced to a single pulse and the subsequent system response. In any case, the reduced amplitude of the oscillations makes difficult to observe them at first glance in the figure. If the function given in (7) is sampled, with a time step $\Delta t = (N\Delta f)^{-1}$, $N = 1024$ and $\Delta f = 0.2\,\text{Hz}$, and transformed to the frequency domain with a DFT, the amplitude spectrum shown in Figure 4(b) is obtained. Only the first half of the samples generated by the DFT is shown in this figure because, as is widely known, the second half is the specular reflection of the first. The amplitude spectrum of the entire signal $g(t)$ is practically superposed on that of the pulse excitation, except for two slight oscillations around the system resonant frequencies at 10 and 30 Hz because the excitation pulse concentrates most of the energy of the function $g(t)$ and the influence of the resonances on the spectrum is practically negligible.

The next step in our analysis procedure is to compress the data logarithmically, expressing them in dBμ, in order to reduce possible differences in amplitude. The compressed amplitude spectrum is shown in Figure 4(c). Now, this spectrum of $g(t)$ can be re-transformed to the time domain using an inverse DFT with zero phase and imposing a real output sequence, since the temporal response of a physical system can be represented by a real function. Figure 4(d) shows this temporal signal, which forms a different signal to the previous $g(t)$ because, although both signals have the same power spectrum, the phases are different. Again, the inverse DFT output is constituted by two halves, one of which is the specular reflection of the other. So, this temporal signal has only 512 independent samples with $\Delta t = 4.9\,\text{ms}$ and only the first 128 samples are shown in Figure 4(d) to highlight the difference between the first samples and the rest of the signal. In the new temporal signal, it is possible to differentiate between an initial pulse related to the excitation signal, which constitutes the early time response, and the later oscillations or late-time response associated with the system response. The early time signal is a pulse centered at $t = 0$ and is directly related to the excitation signal because the Fourier transform of a real time-varying pulse centered at the origin time is another real pulse in the frequency domain centered at the origin

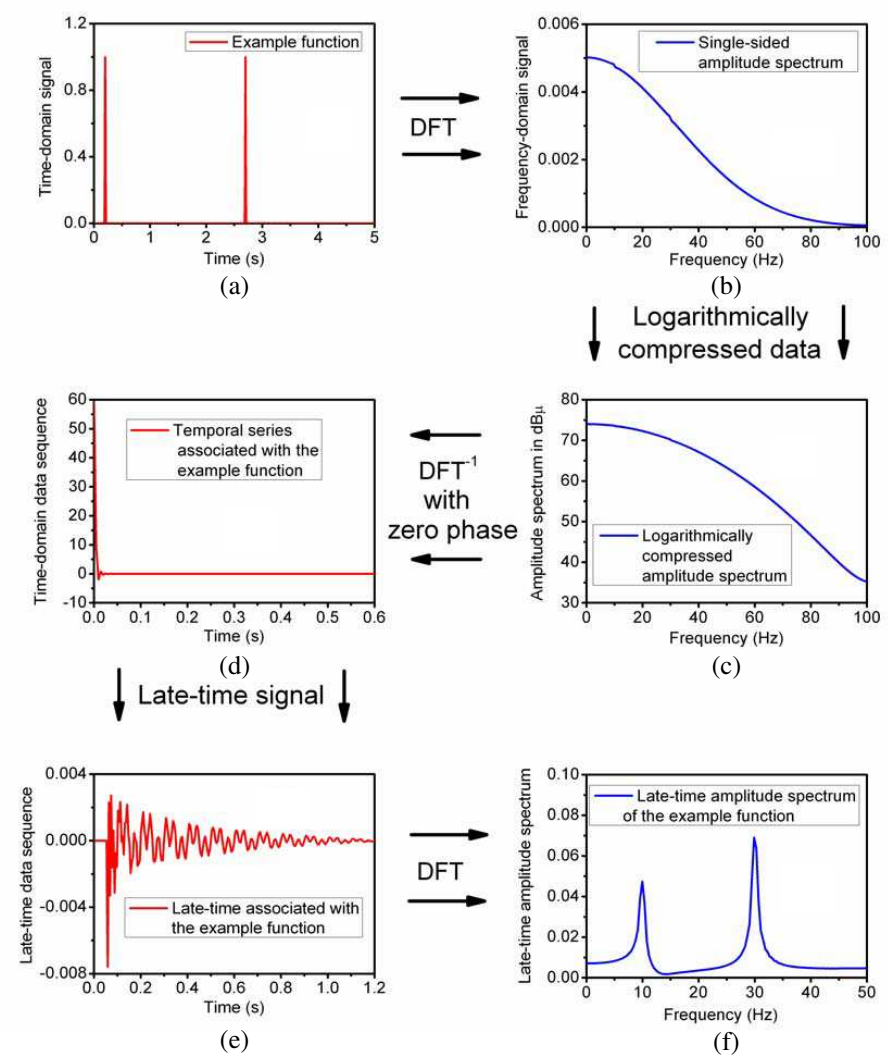

Figure 4. Different stages in the analysis procedure to extract weak resonances.

frequency with null phase. At this stage, we would like to reiterate two points. On the one hand, taking null phase can help obtain the system resonances because the pulses included in the original temporal signal are shifted to the origin of the time, allowing us to distinguish the early time directly related to the excitation and the late time containing information about the system resonances. On the other hand, the

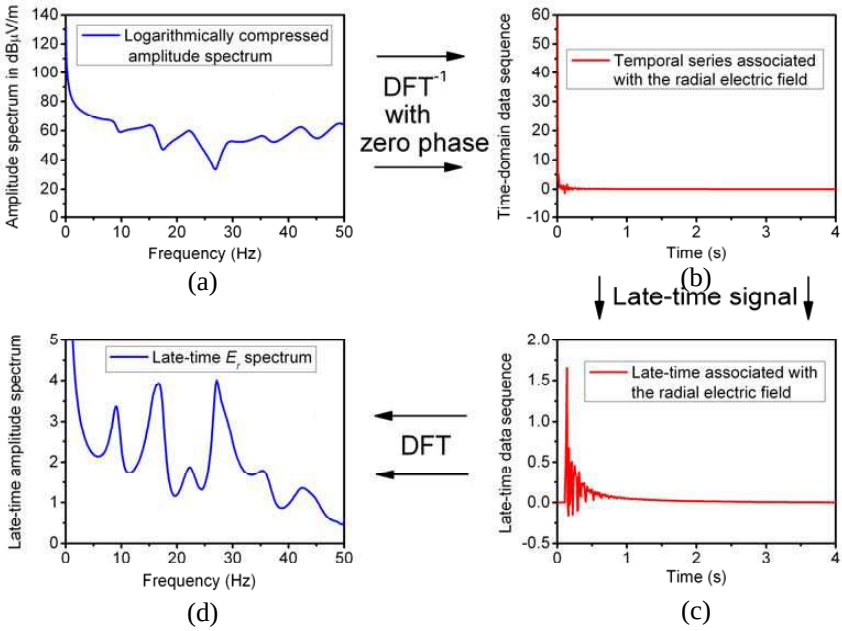

Figure 5. Analysis of the vertical component of electric field in the Earth's electromagnetic cavity.

temporal series obtained via an inverse DFT with zero phase do not represent a real physical magnitude; they are only an intermediate step, a mathematical tool, in the analysis procedure for extracting weak resonances from the response of the physical system. The late-time part of this temporal signal, which is obtained by making the first twelve samples of the entire signal zero, is shown in Figure 4(e). In this case, to annul this number of samples is enough to sufficiently remove the initial exponential pulse. Finally, with a direct DFT of this last temporal series, the late-time spectrum is obtained and shown in Figure 4(f). This last figure is constituted by 128 samples in the frequency domain with $\Delta f = 0.4$ Hz, although the number of samples and the frequency step Δf can be modified by applying the well-known method of "zero padding"; i.e., adding zeroes to the tail of the input temporal signal because the samples in the late time signal oscillate around or tend to zero. The late-time spectrum presents two noticeable peaks at 10 and 30 Hz and, consequently, our analysis was able to identify the weak resonance introduced in the initial analytical function.

The analysis procedure described above with an analytical function is now applied to the numerical signal, obtained by the TLM method, which represents the vertical electric field in Earth's atmosphere as a response to a lightning discharge. Figure 5(a) shows the logarithmically compressed amplitude spectrum for the radial electric field, also shown in Figure 3. This signal may be transformed to the time domain by means of the inverse DFT, assuming zero phases for all frequencies; that is, annulling the arguments in all the complex numbers that represent the spectrum samples. In this case, the frequency domain input signal is constituted by 1044 samples with the frequency step given by the TLM simulation, $\Delta f = 0.096\,\mathrm{Hz}$, and consequently the temporal output is sampled with a time step $\Delta t = 10\,\mathrm{ms}$. The resultant time-domain signal (Figure 5(b)) has two clear regions: an early time at which an important initial pulse is clearly observed and a late time at which a damped oscillation becomes predominant after the initial pulse disappears. With the aim of obtaining and analyzing all the information contained in the late-time response, the early-time response is removed by imposing a zero value for the first twelve samples, giving the signal sketched in Figure 5(c) Finally, Figure 5(d) shows the new Fourier transform, i.e., the DFT of the late-time response. This amplitude spectrum presents an appearance different from the E_r global spectrum shown in Figure 3, because the analysis procedure has modified the oscillations present in the initial spectrum and now clear resonances that correspond with the expected Schumann resonances can be observed. Table 1 includes the peak frequencies obtained after a fit of the E_r late-time spectrum with Lorentzian functions.

5. CONCLUSIONS

Detection of the Schumann resonance frequencies in the atmosphere of a planet or moon is an irrefutable proof of natural electrical activity in the planet or moon's atmosphere. Along with a numerical simulation of the electromagnetic cavity of Earth's atmosphere for the ELF band, our paper presents an analysis of the vertical electric field in order to extract from it the Schumann resonances. The analysis procedure is based on the following idea. The resonances of a system produce oscillations in its temporal response which, depending on the damping ratio, remain visible for more or less time in the response of an under-damped system. These oscillations are merged with the excitation and other possible components that may be included in the signal measured as the temporal response of the system. If the resonances are weak and their amplitudes are low compared to the amplitude of

other components of the total signal, their existence can go unnoticed in a global analysis of the entire signal. However, if the temporal signal has a low-amplitude oscillating tail due to the non-existence of excitation in this part of the signal, then it might be possible to find the system's natural resonances by analyzing the oscillating tail or late-time response. Thus, to analyze a temporal signal obtained via an inverse DFT of the spectra with phase zero could be of great help because all the pulses included in this signal would be automatically transferred to the origin of the signal, leaving the tail of the signal free, since the Fourier transform of a real time-varying pulse centered at the origin time is another pulse in the frequency domain centered at the origin frequency with null phase. The above process, applied to the vertical component of electric fields obtained with the TLM method, generates a series of Schumann resonances with values close to those supplied by the horizontal magnetic field and the experimental ones.

ACKNOWLEDGMENT

This work was partially supported by the Ministerio de Ciencia e Innovación of Spain and Consejería de Innovación, Ciencia y Empresa of Andalusian Government under projects with references FIS2010-15170 and PO7-FQM-03280, co-financed with FEDER funds of the European Union. The authors also thank B. Lamplugh for her help in preparing the manuscript.

REFERENCES

1. Tinsley, B. A. and L. Zhou, "Initial results of a global circuit model with variable stratospheric and tropospheric aerosols," *J. Geophys. Res.*, Vol. 111, No. D16205, 1–23, 2006.
2. Makino, M. and T. Ogawa, "Quantitative estimation of global circuit," *J. Geophys. Res.*, Vol. 90, No. D4, 5961–5966, 1985.
3. Sentman, D. D., "Schumann resonances," *Handbook of Atmospheric Electrodynamics*, Vol. 1, edited by H. Volland, 267–295, CRC Press, Boca Raton, Fla., 1995.
4. Morente, J. A., J. A. Portí, A. Salinas, G. J. Molina-Cuberos, H. Lichtenegger, B. P. Besser, and K. Schwingenschuh, "Do Schumann resonance frequencies depend on altitude?," *J. Geophys. Res.*, Vol. 109, No. 05306, 1–6, 2004.
5. Christian, H. J., R. J. Blakeslee, D. J. Boccippio, W. L. Boeck, D. E. Buechler, K. T. Driscoll, S. J. Goodman, J. M. Hall, W. J. Koshak, D. M. Mach, and M. F. Stewart, "Global frequency

and distribution of lightning as observed from space by the optical transient detector," *J. Geophys. Res.*, Vol. 108, No. 1, 1–15, 4005, 2003.

6. Barr, R., D. L. Jones, and C. J. Rodger, "ELF and VLF radio waves," *J. Atmos. Sol. Terr. Phys.*, Vol. 62, Nos. 17–18, 1689–1718, 2000.
7. Balanis, C. A., *Advanced Engineering Electromagnetics*, John Wiley & Sons, Inc., Hoboken, N.J., 1989.
8. Poeverlein, H., "Resonance of the space between Earth and ionosphere," *J. Res. NBS (Radio Prop.)*, Vol. 65, No. 5, 465–473, 1961.
9. Bliokh, P. V., Y. P. Galyuk, E. M. Hünninen, A. P. Nikolaenko, and L. M. Rabinovich, "Resonance effects in the Earth-ionosphere cavity," *Radiophys. Quant. Electron.*, Vol. 20, No. 4, 339–345, 1977.
10. Nikolaenko, A. P. and L. M. Rabinovich, "Possible global electromagnetic resonances on the planets of the solar system," *Cosmic Res.*, Vol. 20, No. 1, 67–71, 1982.
11. Sentman, D. D., "Schumann resonance spectra in a two-scale-height Earth-ionosphere cavity," *J. Geophys. Res.*, Vol. 101, No. 5, 9479–9487, 1996.
12. Morente, J. A., J. A. Portí, B. P. Besser, A. Salinas, H. I. M. Lichtenegger, E. A. Navarro, and G. J. Molina-Cuberos, "A numerical study of atmospheric signals in the Earth-ionosphere electromagnetic cavity with the transmission line matrix method," *J. Geophys. Res.*, Vol. 111, No. 10305, 1–13, 2006.
13. Schumann, W. O., "Über die strahlungslosen Eigenschwingungen einer leitenden Kugel, die von einer Luftschicht und einer Ionosphärenhülle umgeben ist," *Z. Naturforsch. A*, Vol. 7, 149–154, 1952.
14. Besser, B. P., "Synopsis of the historical development of Schumann resonances," *Radio Sci.*, Vol. 42, No. RS2S02, 1–20, 2007.
15. Wait, J. R., *Geo-electromagnetism*, Academic Press, London, 1982.
16. Budden, K. G., *The Propagation of Radio Waves: The Theory of Radio Waves of Low Power in the Ionosphere and Magnetosphere*, Cambridge Univ. Press, New York, 1985.
17. Nickolaenko, A. P. and M. Hayakawa, *Resonances in the Earth-ionosphere Cavity*, Springer, New York, 2002.
18. Balser, M. and C. A. Wagner, "Observations of Earth-ionosphere

cavity resonances," *Nature*, Vol. 188, No. 4751, 638–641, 1960.

19. Williams, E. R., "The Schumann resonance: A global tropical thermometer," *Science*, Vol. 256, No. 5060, 1184–1187, 1992.
20. Sentman, D. D., "Approximate Schumann resonance parameters for a two-scale-height ionosphere," *J. Atmos. Sol. Terr. Phys.*, Vol. 22, No. 1, 35–46, 1990.
21. Rycroft, M. J., A. Odzimek, N. F. Arnold, M. Füllekrug, A. Kulak, and T. Neuber, "New model simulations of the global atmospheric electric circuit driven by thunderstorms and electrified shower clouds: The roles of lightning and sprites," *J. Atmos. Sol. Terr. Phys.*, Vol. 69, 2485–2509, 2007.
22. Cummer, S. A., "Modeling electromagnetic propagation in the Earth-ionosphere waveguide," *IEEE Trans. Antennas and Propag.*, Vol. 48, No. 9, 1420–1429, 2000.
23. Hayakawa, M. and T. Otsuyama, "FDTD analysis of ELF wave propagation in inhomogencous subionospheric waveguide models," *Appl. Computational Electromagnetics Soc. J.*, Vol. 17, No. 3, 239–244, 2002.
24. Otsuyama, T., D. Sakuma, and M. Hayakawa, "FTDT analysis of ELF wave propagation and Schumann resonanace for a subionopheric waveguide model," *Radio Sci.*, Vol. 38, No. 6, 1103, 2003.
25. Yang, S., Y. Chen, and Z.-P. Nie, "Simulation of time modulated linear antenna arrays using the FDTD method," *Progress In Electromagnetics Research*, Vol. 98, 175–190, 2009.
26. Zhang, Y.-Q. and D.-B. Ge, "A unified FDTD approach for electromagnetic analysis of dispersive objects," *Progress In Electromagnetics Research*, Vol. 96, 155–172, 2009.
27. Christopoulos, C., *The Transmission-line Modeling Method: TLM*, IEEE/OUP Press, New York, 1995.
28. Schlegel, K. and M. Füllekrug, "Schumann resonance parameter changes during high-energy particle precipitation," *J. Geophys. Res.*, Vol. 104, No. 5, 10111–10118, 1999.
29. Plonus, M. A., *Applied Electromagnetics*, McGraw-Hill, New York, 1978.
30. De Cogan, D., S. H. Pulko, and W. J. O'Connor, *Transmission Line Matrix in Computational Mechanics*, CRC Press, Boca Raton, Fla., 2005.
31. Johns, P. B., "A symmetrical condensed node for the TLM method," *IEEE Trans. Microwave Theory Tech.*, Vol. 35, No. 4, 370–377, 1987.

32. Morente, J. A., G. J. Molina-Cuberos, J. A. Portí, B. P. Besser, A. Salinas, K. Schwingenschuch, and H. Lichtenegger, "A numerical simulation of Earth's electromagnetic cavity with the transmission line matrix method: Schumann resonances," *J. Geophys. Res.*, Vol. 108, No. 5, 1–11, 2003.
33. Sukhorukov, A. I., "Lightning transient fields in the atmosphere-low ionosphere," *J. Atmos. Terr. Phys.*, Vol. 58, No. 15, 1711–1720, 1996.
34. Ogawa, T., "Lightning currents," *Handbook of Atmospheric Electrodynamics*, Vol. 1, edited by H. Volland, 93–136, CRC Press, Boca Raton, Fla., 1995.
35. Gómez, R. and J. A. Morente, "Analysis of electric quadrupole radiation in the time domain: Application to large current radiators," *Int. J. Electron.*, Vol. 58, No. 6, 921–931, 1985.
36. Sentman, D. D., "Magnetic elliptical polarization of Schumann resonances," *Radio Science*, Vol. 22, No. 4, 595–606, 1987.
37. Mushtak, V. C. and E. Williams, "ELF propagation parameters for uniform models of the Earth-ionosphere waveguide," *J. Atmos. Sol. Terr. Phys.*, Vol. 64, No. 18, 1989–2001, 2002.
38. Gharsallah, N., E. J. Rothwell, K. Chen, and D. P. Nyquist, "Identification of the natural resonance frequencies of a conducting sphere from a measured transient response," *IEEE Trans. Antennas and Propag.*, Vol. 38, No. 1, 141–143, 1990.